Student Paper

Atomistic simulations for SiGe pMOS devices – Bandstructure to Transport

Saumitra R Mehrotra[a], Abhijeet Paul[a], Mathieu Luisier[a] and Gerhard Klimeck[a]

[a] *Department of Electrical & Computer Engineering, Purdue University, USA, smehrotr@purdue.edu,*

Introduction: SiGe pMOSFETs show considerable improvements in device performance due to the smaller hole effective mass exhibited by Ge.Further improvement in device performance can be obtained by growing pseudomorphically compressively strained SiGe on Si. Despite a lattice mismatch of ~4% between Si and Ge, researchers have been recently able to fabricate ultrathin body and nanowire pMOSFETs with high Ge concentrations and compressive strain [1,2]. Strained SiGe pMOS devices are being considered as one of the designs for the ultimate pMOS [3]. To treat quantum confined devices atomistic modeling becomes important. Here we present tight-binding (TB) based bandstructure calculations in the virtual crystal approximation (VCA) for bulk relaxed SiGe and strained SiGe on (100) Si benchmarked against experimental data.

Method: *VCA of Si and Ge [4]*. The $Si_{1-x}Ge_x$ two center integals between two neighbor atoms are calculated as $V_{SiGe}=(1-x).(d_{Si}/d_{SiGe})^{\eta}V_{Si}+x.(d_{Ge}/d_{SiGe})^{\eta}V_{Ge}$ [5]. Fig. 1 shows the resulting relaxed bulk bandstructure of SiGe with varying Ge concentration. Crossover in conduction band at ~85% Ge from X valley to L valley is correctly captured in our TB VCA model. Fig. 2 shows the band edge variation with Ge% for compressively strained case of SiGe/(100)Si. Compressively strained SiGe shows a band gap reduction which is entirely due to shift in valence band edge Fig. 3 shows the bandgap of strained and relaxed SiGe. Our calculations show good agreement with experimental data. As the Ge concentration increases, the hole DOS effective mass of SiGe becomes smaller, as shown in Fig. 4. Compressive strain leads to a splitting of the Heavy Hole (HH) and Light Hole (LH) states at the Γ point. This splitting leads to a reduction of the interaction (warping) between the HH and LH bands. This effect is manifested in a decrease of the HH DOS effective mass and a slight increase of the LH DOS effective mass (Fig.4). Finally, Fig. 5 shows the electron masses for the X (100) and L (111) valleys of relaxed and strained SiGe. Electron masses do not exhibit large changes in both cases.

Application: We have used our TB VCA model described above and a ballistic top-of-the-barrier (TOB) transport approach to simulate a SiGe nanowire pMOSFET (Fig. 6) & benchmarked with recent experimental data [2]. Comparing our simulation results shows a ballisticity ratio of about 82% for the 13 nm diameter <100> oriented SiGe nanowire device. This is consistent with the high ballisticity factor predicted (~ 0.9) in gate all around nanowire devices [13].

Conclusion: We have presented an atomistic approach for treating SiGe pMOSFET devices. A novel tight-binding bandstructure parametrization has been developed and validated for bulk SiGe. It has then been applied to ballistic simulation of quantum confined SiGe nanowire pMOS and compared to experimental result.

Acknowledgement: MSD/MARCO and NSF for financial support. NCN for providing computational resources.

References

[1] C. N. Chleirigh et. al., "Thickness Dependence of Hole Mobility in Ultrathin SiGe-Channel p-MOSFETs," *Electron Devices, IEEE Transactions on*, vol.55, no.10, pp.2687-2694, Oct. 2008. [2] Y. Jiang et. al., "Ge-rich (70%) SiGe nanowire MOSFET fabricated using pattern-dependent Ge-condensation technique," *IEEE Electron Device Lett.*, vol. 29, no. 6, pp. 595–598, Jun. 2008. [3] S Takagi et al, "Carrier-Transport-Enhanced Channel CMOS for Improved Power Consumption and Performance," *Electron Devices, IEEE Transactions on* , vol.55, no.1, pp.21-39, Jan. 2008. [4] T. B. Boykin, G. Klimeck and F. Oyafuso, "Valence Band Effective-Mass Expressions in the sp3d5s* Empirical Tight-Binding Model Applied to a Si and Ge Parametrization," *Phys. Rev. B,* vol. 69, 115201/1-10, Mar. 2004. [5] T. B. Boykin et al, "Diagonal parameter shifts due to nearest-neighbor displacements in empirical tight-binding theory," *Phys. Rev. B, Condens. Matter*, vol. 66, no. 12, p. 125 207, Sep. 2002. [6] Semicondctors: Group IV Elements and III-V Compunds, edited by O. Madelung (Springer,New York, 1991) [7] J. F. Morar, P. E. Batson, and J. Tersoff, "Heterojunction band discontinuity in Si-Ge alloys using spatially resolved electron-energy-loss spectroscopy," *Phys. Rev. B,* vol. 47, pp. 4107-4110, 1993. [8] L. Yang et. al. "Si/SiGe heterostructure parameters for device simulations," *Semicond. Sci. Technol.*, vol. 19, pp. 1174, Oct. 2004. [9] J. Hoyt, et. al, "Evaluation of the valence band discontinuity of $Si/Si_{1-x}Ge_x/Si$ heterostructures by application of admittance spectroscopy to MOS capacitors," *Electron Devices, IEEE Transactions on*, vol.45, no.2, pp.494-501, Feb 1998. [10] D. J. Robbins et. al., "Near-band-gap photoluminescence from

pseudomorphic $Si_{1-x}Ge_x$ single layers on silicon," J. Appl. Phys. 71, 1407, 1992. [11] D. V. Lang, et. al., "Measurement of the band gap of GexSi(1-x)/Si strained-layer heterostructures," Appl. Phys. Lett. 47, 1333, 1985. [12] D. Dutartre, "Excitonic photoluminescence from Si-capped strained Si1-xGex layers," *Phys Rev B,* vol. 44, no. 20, pp 11525, Nov. 1991. [13] A. Khakifirooz and D. A. Antoniadis, "Transistor performance scaling:The role of virtual source velocity and its mobility dependence," in *IEDM Tech. Dig.*, pp. 667–670, 2006.

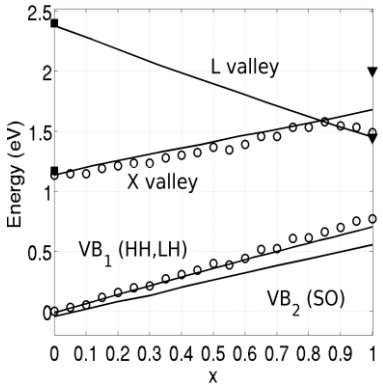

Figure 1 Calculated bandedges for relaxed bulk $Si_{1-x}Ge_x$ with increasing Ge%. Experimental references are from Madelung [6] (■) for Si and (▼) for Ge band edges. Morar [7] conduction band edge data(○) is shown. Valence band reference (○) calculated by subtracting Morar data with band gap data from Asenov Eg target [8].

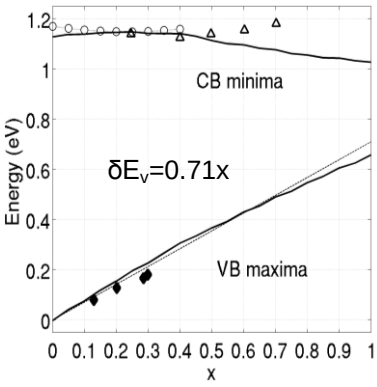

Figure 2 Calculated bandedges for strained $Si_{1-x}Ge_x$ /(100)Si with increasing Ge%. Hoyt (♦) [9] results for valence band shift. Straight line (dotted) represents the Asenov [8] target for ΔE_v. Robbins (○) [10] and Lang (Δ) [11] data for conduction band.

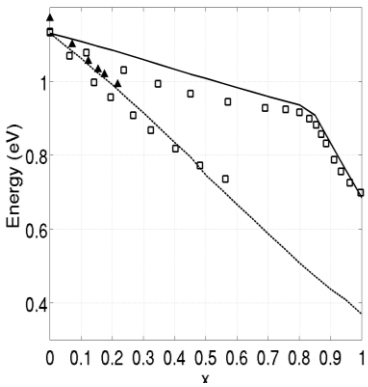

Figure 3 Bandgap results calculated for compressively strained $Si_{1-x}Ge_x$/(100)Si (dotted) and relax $Si_{1-x}Ge_x$ (solid). Lang data [11] (□) for strained and relaxed cases are plotted. Dutartree [12] (▲) low temperature data for strained case is shown.

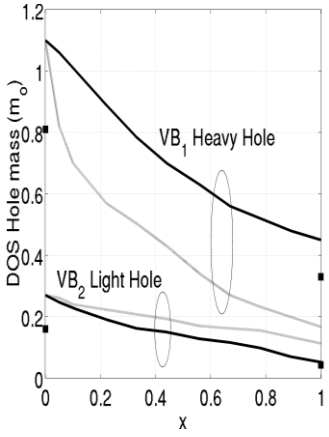

Figure 4 Calculated density of states (DOS) mass for heavy and light holes for relax $Si_{1-x}Ge_x$ (solid) and strained $Si_{1-x}Ge_x$/(100)Si (dotted) cases. DOS mass for each band computed at 3/2 kT (eV) from their respective band maxima at 300K. Experimental (■) data from Madelung [6] for relax case.

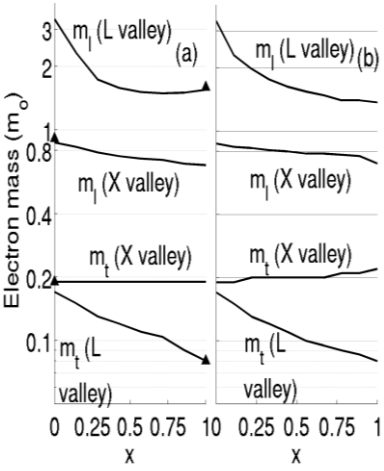

Figure 5 Calculated transverse (m_t) and longitudinal (m_l) electron masses for X (100) and L (111) valleys for (a) relax $Si_{1-x}Ge_x$ case and (b) strained $Si_{1-x}Ge_x$/(100) Si. Experimental data from Madelung [6].

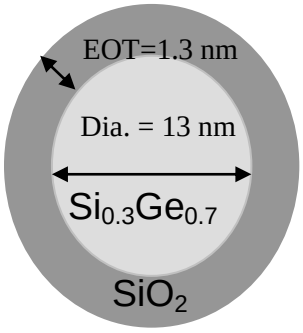

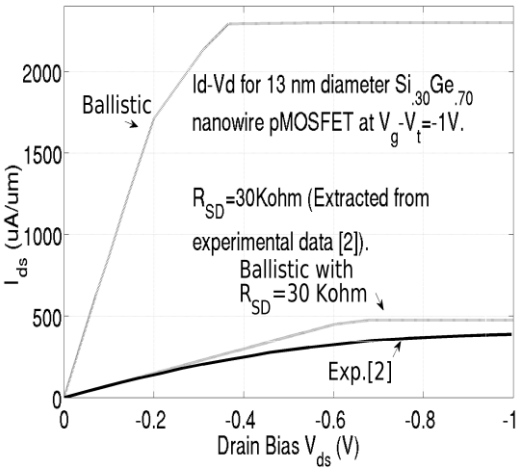

(a) **(b)**

Figure 6 (a) Cross-section of the simulated device as per. Dimensions from exp. data [2] **(b)** Id-Vd characteristics for <100> $Si_{0.3}Ge_{0.7}$ nanowire pMOSFET – shown for exp. (solid) [2] and simulated (dotted) devices. Ballistic currents computed using Top of the Barrier transport model. Computed ballistic R_{CH}=2.79 kΩ. and ballisiticity ratio BR~82% with Ion (ballistic) ~474μA/μm and Ion (experimental) ~388 μA/μm (currents normalized to perimeter) for ON state. Ballistic current adjusted for R_{SD} =30kΩ, extracted from experimental data.